HHS Public Access

Author manuscript

Sci Transl Med. Author manuscript; available in PMC 2016 July 28.

Published in final edited form as:

Sci Transl Med. 2015 September 16; 7(305): 305ra147. doi:10.1126/scitranslmed.aac4441.

Sparing the region of the salivary gland containing stem cells preserves saliva production after radiotherapy for head and neck cancer

Peter van Luijk[1,*], **Sarah Pringle**[1,2], **Joseph O. Deasy**[3], **Vitali V. Moiseenko**[4], **Hette Faber**[1,2], **Allan Hovan**[5], **Mirjam Baanstra**[1,2], **Hans P. van der Laan**[1], **Roel G. J. Kierkels**[1], **Arjen van der Schaaf**[1], **Max J. Witjes**[6], **Jacobus M. Schippers**[1,7], **Sytze Brandenburg**[8], **Johannes A. Langendijk**[1], **Jonn Wu**[5], and **Robert P. Coppes**[1,2,*]

[1]Department of Radiation Oncology, University Medical Center Groningen, University of Groningen, 9700 RB Groningen, Netherlands [2]Department of Cell Biology, University Medical Center Groningen, University of Groningen, 9713AV Groningen, Netherlands [3]Radiation Oncology, Washington University School of Medicine, St. Louis, MO 63110, USA [4]Department of Radiation Medicine and Applied Sciences, University of California San Diego, La Jolla, CA 92093, USA [5]British Columbia Cancer Agency–Vancouver Centre, Vancouver, British Columbia V5Z 4E6, Canada [6]Department of Oral and Maxillofacial Surgery, University Medical Center Groningen, University of Groningen, 9700 RB Groningen, Netherlands [7]Accelerator Department, Paul Scherrer Institut, CH-5212 Villigen, Switzerland [8]KVI Center for Advanced Radiation Technology, University of Groningen, 9747 AA Groningen, Netherlands

Abstract

Each year, 500,000 patients are treated with radiotherapy for head and neck cancer, resulting in relatively high survival rates. However, in 40% of patients, quality of life is severely compromised because of radiation-induced impairment of salivary gland function and consequent xerostomia (dry mouth). New radiation treatment technologies enable sparing of parts of the salivary glands. We have determined the parts of the major salivary gland, the parotid gland, that need to be spared to ensure that the gland continues to produce saliva after irradiation treatment. In mice, rats, and humans, we showed that stem and progenitor cells reside in the region of the parotid gland containing the major ducts. We demonstrated in rats that inclusion of the ducts in the radiation field led to loss of regenerative capacity, resulting in long-term gland dysfunction with reduced saliva production. Then we showed in a cohort of patients with head and neck cancer that the

[*]Corresponding author. p.van.luijk@umcg.nl (P.v.L.); r.p.coppes@umcg.nl (R.P.C.).

SUPPLEMENTARY MATERIALS

www.sciencetranslationalmedicine.org/cgi/content/full/7/305/305ra147/DC1 Materials and Methods Table S1. Planning objectives.

Author contributions: P.v.L. and R.P.C. designed the study. P.v.L., H.F., J.M.S., and S.B. performed the animal irradiation and follow-up experiments. S.P., H.F., M.B., and R.P.C. performed the immunohistochemistry and morphological studies. P.v.L. and R.P.C. analyzed the animal data. V.V.M., A.H., and J.W. performed the clinical prospective cohort study at the British Columbia Cancer Agency. P.v.L., A.v.d.S., and J.O.D. analyzed the clinical prospective cohort study. P.v.L., H.P.v.d.L., R.G.J.K., and J.A.L. performed the treatment planning comparison study. P.v.L. and A.v.S. estimated the clinical impact. M.J.W. provided biopsies. All authors critically read and edited the manuscript.

Competing interests: The authors declare that they have no competing interests.

radiation dose to the region of the salivary gland containing the stem/progenitor cells predicted the function of the salivary glands one year after radiotherapy. Finally, we showed that this region of the salivary gland could be spared during radiotherapy, thus reducing the risk of post-radiotherapy xerostomia.

INTRODUCTION

Most cancer patients receive radiotherapy as part of their treatment. When using radiotherapy, irradiation of normal tissue, in particular tissue close to the tumor, is unavoidable. This leads to tissue damage, often resulting in complications (1). An example of this is severe hyposalivation, which is a very common and often irreversible side effect resulting from radiotherapy of tumors in the head and neck area. Worldwide, 500,000 patients are treated for head and neck cancer annually. Quality of life in many of the survivors is severely compromised. Hyposalivation and its related complaints including xerostomia (dry mouth syndrome) lead to an increased susceptibility to oral infections and dental caries, impeded swallowing and food mastication, impaired taste and speech, and nocturnal oral discomfort, all of which have a major detrimental impact on health-related quality of life (2–7). Strategies to prevent radiation-induced salivary gland dysfunction and consequent xerostomia include the use of protective medications (8–11), surgical relocation of the submandibular gland, and minimization of the radiation dose administered to the major salivary glands [the parotid gland (4, 12–15) and the submandibular gland (16)]. The current approach to spare the parotid gland aims to minimize the radiation dose to the entire organ (3, 14, 15, 17–19). Although this approach has indeed reduced the incidence of xerostomia, about 40% of patients still suffer from symptoms after radiotherapy (15). The main difference between conventional and parotid gland–sparing radiotherapy is that the former results in persistent xerostomia, whereas the latter results in partial recovery over time (15, 19). This is consistent with the observation that the damaged parotid gland is capable of regaining some of its function in the first 2 years after radiotherapy (20, 21). This suggests that the parotid gland contains cells capable of regenerating damaged tissue. The presence of parotid gland stem cells has been documented in mice treated with keratinocyte growth factor, which increased the number of surviving stem/progenitor cells and allowed improved long-term regeneration of the salivary glands (22). Moreover, mouse submandibular gland function could be rescued from ablative radiation doses by the transplantation of tissue-specific stem cells (23).

The effect of radiation dose on the rat parotid gland was shown to depend on where the dose was targeted (24). Irradiation of the caudal parts of the rat parotid gland resulted in tissue degeneration restricted to the irradiated tissue and regeneration outside the irradiated area, whereas irradiation of the cranial 50% of the gland caused degeneration of the entire gland including the shielded parts (24, 25). This indicates that a specific region of the gland may be more sensitive to the detrimental effects of radiation. Modern high-precision radiotherapy techniques such as intensity-modulated radiotherapy (IMRT) and particle therapy are able to deposit a dose with such accuracy that it is conceivable that specific regions of the parotid gland could be spared. However, current knowledge about the potential role of anatomical substructures in the regeneration of the parotid gland after irradiation is insufficient to allow

clinical decision-making. Thus, to achieve clinical benefit, it is imperative that these stem cell–containing regions are identified.

Here, we determined the distribution of mouse, rat, and human stem/progenitor cells in the parotid gland, and elucidated their regenerative capacity and assessed whether they could be spared specifically in patients. We show that different parts of the gland differed in regenerative capacity and that irradiation of the region containing the largest number of stem/progenitor cells resulted in the strongest adverse outcome. We documented in patients that the dose to the stem cell–containing region of the human salivary gland was highly predictive of parotid gland dysfunction after radiotherapy. Our analysis showed that the radiation dose to the region responsible for functional recovery could be reduced substantially using current radiotherapy technology. We demonstrated that this strategy could reduce radiotherapy-induced parotid gland dysfunction in head and neck cancer patients. This strategy is now being tested in an ongoing prospective randomized clinical trial.

RESULTS

Non-uniform distribution of stem/progenitor cells in salivary gland

To investigate the distribution of stem/progenitor cells in the human parotid gland, we first looked at the distribution of cells expressing c-Kit, a known salivary gland stem/progenitor cell marker (23). c-Kit$^+$ cells were found exclusively within the ducts of human parotid glands (Fig. 1A) as has been found for rat (Fig. 1B) and mouse parotid glands (fig. S2) and mouse submandibular glands (23). The intensity and number of c-Kit$^+$ cells were higher in the larger excretory ducts (Fig. 1B, inset) compared to areas with smaller ducts, and almost disappeared at the exterior of the gland. Moreover, when outer and center samples (Fig. 1C) were assessed using tissue FAXS [a microscopy-based fluorescence-activated cell sorting (FACS)–like method for quantitating cells in tissue], the number of high-intensity c-Kit$^+$ cells was greater in the center part of the parotid gland (Fig. 1, C and D). This indicates that the distribution of cells expressing c-Kit in mouse, rat, and human parotid glands is not uniform.

Next, we assessed the in vitro regenerative capacity of the rat parotid gland using a sphere-forming assay. Salispheres, spheres derived from the salivary tissue, can be grown from dispersed salivary glands (23). They are enriched in cells that express c-Kit and other stem cell markers, and are capable of rescuing salivary gland function after radiation damage (23, 26). This sphere-forming assay reflects the regenerative capacity of the salivary glands (22). However, accurately determining the location of substructures with regenerative capacity in the small glands of mice is difficult, so we developed a similar assay for the rat parotid gland. Dissociation and culturing of rat parotid gland cells resulted in the formation of spheres (Fig. 1E). These spheres were capable of forming secondary spheres from single cells that could differentiate into salivary gland–like organoids in three-dimensional (3D) matrix culture (Fig. 1F) similar to those from the mouse submandibular gland (27). The number of spheres formed per milligram of tissue was greater for tissue obtained from the central than from the outer parts of the rat parotid gland (Fig. 1, G and H). These results

show that rat parotid gland stem/progenitor cells are not evenly distributed but are more abundant in the central part compared to the exterior part of the parotid gland.

Rat parotid gland regeneration after irradiation

To test whether the central area of the parotid gland contains cells that allow long-term recovery of function, we specifically irradiated small subsections of the rat parotid gland (Fig. 2, A to E) using a high-precision proton irradiation setup (25). High radiation doses are known to prevent any regeneration in that part of the gland (24, 28). To confirm our previous findings obtained after photon irradiation (24, 28), we first irradiated 50% of the rat parotid gland and measured saliva flow rates for up to 1 year after irradiation. Indeed, irradiation of the caudal 50% of the parotid gland resulted in loss of less than 50% saliva production (less than proportional) (Fig. 2A). In contrast, irradiation of the cranial 50% of the parotid gland resulted in a more than proportional and progressive loss of saliva flow rate, indicating an inability to restore saliva secretion. To investigate whether this was due to a lack of regenerative competence, the morphology of the gland was analyzed 1 year after irradiation (Fig. 3). Two types of morphology could be distinguished: intact, showing abundant acini and normal ducts (Fig. 3A), or degenerative, lacking acinar cells with an increased number of ducts and fibrosis (Fig. 3B). These characteristic morphologies could easily be discerned when assessing whole-gland preparations (Fig. 3, C to E). Figure 3C shows a section of a gland obtained from a non-irradiated control rat, with intact lobes and normal acinar tissue. Irradiation of the caudal 50% of the rat parotid gland led to clear damage to the irradiated lateral lobe and the caudal parts of the ventral lobe, but no visible damage elsewhere (Fig. 3D). In contrast, irradiation of the cranial 50% of the gland resulted in complete degeneration of the gland, including the non-irradiated parts (Fig. 3E). Therefore, clear differences in regenerative capacities are present between the caudal and cranial regions of the gland.

To further pinpoint the location of the critical region, we irradiated various differently sized and located subsections of the rat parotid gland (Fig. 2, A to D). In these experiments, responses were classified as “proportional” if the relative loss of saliva production did not exceed the relative irradiated volume (for example, after irradiation of the caudal 50% of the gland; Fig. 2A, cyan curve) or “more than proportional” if the loss exceeded the relative size of the irradiated volume (for example, after irradiation of the cranial 50% of the gland; Fig. 2A, blue curve). An overview of responses is shown in Fig. 2E. Irradiation of 25% of the rat parotid gland did not result in sustained loss of function (Fig. 2, B and E, gray lines), indicating that the critical region is larger than 25% of the gland. The most radiosensitive regions shared a small subvolume (between the stippled lines), which was excluded from fields that resulted in a less-than-proportional response. Indeed, this region was located centrally at the junction of the ventral, dorsal, and lateral lobes, supporting the hypothesis that the long-term regenerative capacity of the salivary glands resides in the region of the gland that is known to contain the majority of stem/progenitor cells.

Next, we determined the relation between ablated volume and damaged volume. For each irradiated volume, the fraction of each lobe showing degeneration was scored by measuring the area of tissue on the slide that showed normal (Fig. 3A) or degenerative (Fig. 3B)

morphology; this was then related to the irradiated fraction (Fig. 4B). When the critical volume was not irradiated, the damaged fraction corresponded to the irradiated fraction of each lobe (Figs. 3, C and D, and 4C). In contrast, if the critical region was irradiated, the damaged fraction did not depend on the irradiated fraction (Figs. 3, C and E, and 4D).

The regenerative capacity of the human parotid gland

To test whether human salivary gland regeneration depends on regional dosage, 74 patients were treated with radiotherapy and whole-mouth stimulated saliva was measured. These patients were diagnosed with head and neck cancer with no tumor involvement in the salivary glands (29). On the basis of availability of follow-up data, they were selected from a prospective cohort study performed at the British Columbia Cancer Agency in Vancouver, Canada.

Using a 10-fold cross-validation analysis, we determined the subvolume of gland that had a dose associated most strongly with saliva production 1 year after radiotherapy. This subvolume was located near the dorsal edge of the mandible (Fig. 5A and figs. S3 to S12). This is the region where the first branching of Stensen's duct occurs, which is consistent with data from rat and mouse parotid glands reported in Figs. 1 to 4. Moreover, the radiotherapy dose to this region was consistently found to predict posttreatment function more accurately than the conventional mean dose to the entire gland in a fivefold cross-validation procedure (Fig. 5, B and C, and Supplementary Methods). Finally, only cells from patient biopsies taken from this region could be grown in the sphere assay (figs. S13 and S14). These results indicate that the dosage to the region containing major ducts correlates with clinical outcome.

Reducing radiotherapy-induced human parotid gland dysfunction

These data may be immediately applicable to reduce the side effects during radiation therapy for head and neck tumors. Therefore, we determined the potential clinical gain that could be achieved by avoiding irradiation of this sensitive region. To this end, we generated two treatment plans in 22 patients. The first plan was based on current standard treatment optimization, that is, IMRT (see Supplementary Methods). In such optimization, maximum acceptable doses/irradiated volumes or mean doses (dose constraints) were specified. Subsequently, the mean dose to the parotid glands was minimized. In the second treatment plan, the dose to the identified critical region was minimized.

Figure 6A shows a slice of a computed tomography (CT) scan of a patient through the center of the critical region (red circle) of the parotid gland (green contour). The dose distribution shown is the result of minimizing the mean dose to the whole parotid gland. This results in irradiating a large volume of the gland at intermediate dose levels. Specific minimization of the mean dose to the critical region (for example, Fig. 6B) generally resulted in a redistribution of dose within the parotid gland (Fig. 6, B to D). Although the level of dose reduction varied between individual patients, this indicated that even in patients where sparing of the whole parotid gland is not feasible, the dose to the stem cell–containing region can be reduced. Figure 6C illustrates the dose to the critical region after optimization against the dose using a standard treatment technique. On the basis of the relation between

dose to the critical region and loss of parotid gland function shown in Fig. 5D, this was predicted to result in an improvement in parotid gland function (Fig. 6E).

In summary, radiotherapy-induced parotid gland dysfunction depended on the radiotherapy dose administered to the region containing the stem/progenitor cells responsible for long-term regeneration. The dose to this area could be reduced without compromising other treatment planning objectives.

DISCUSSION

After radiotherapy for head and neck cancer, damage to the salivary glands often leads to severe complications, which reduce the quality of life of patients (2). The current approach to spare salivary gland function is to minimize the mean dose to the entire parotid gland (3, 14, 15, 17, 18). However, this dose reduction is generally insufficient to prevent hyposalivation. Here, we demonstrated in mice and rats that salivary gland stem and progenitor cells are predominantly located in the major ducts. This was demonstrated by the finding of a non-uniform distribution of cells expressing c-Kit in mouse, rat, and human parotid glands. It could be argued that other stem cell markers alone or coexpressed with c-Kit may represent a more valid stem cell population (27, 30). However, these markers (CD24/CD29) either stained too heavily or stained only a very limited number of c-Kit coexpressing cells of the gland ductal areas in the three species investigated. Moreover, it has been shown that the c-Kit$^+$ population is most potent in tissue regeneration given that only 100 cells can rescue the irradiated murine salivary gland (23). Localized irradiation of the major parotid gland ducts resulted in radiation-induced parotid gland dysfunction. In patients with head and neck cancer, we found that the radiation dose to a subvolume of the salivary glands in which the major ducts resided and from which the excretory duct emerged predicted parotid gland dysfunction.

We also showed that specific attempts to reduce the radiation dose to the region containing the major ducts were predicted to improve posttreatment parotid gland function compared to standard treatments. Whether such optimization strategies will eventually result in less xerostomia among patients remains to be determined in a prospective randomized trial. The extent to which sparing of the region containing the major ducts is possible may differ depending on the irradiation technology used. Data about which part of the salivary gland should be spared, as we have provided here, will help in choosing between existing technologies and may inspire technology improvement.

The finding in patients that the irradiation dose to the structures containing the parotid gland stem cells determines the severity of parotid gland dysfunction after radiation treatment confirms the important role of these stem cells in long-term salivary gland function. It also suggests that autologous transductal stem cell transplantation may be a viable treatment strategy in patients where sparing this specific subvolume of the salivary glands is not feasible.

Interestingly, for posttreatment parotid gland function, the improvement in prediction performance of the critical region model was relatively small compared to the prediction

performance of a model based on mean dose to the whole gland. There could be several reasons for this. First, the mean dose to the parotid gland correlated with the dose to the stem cell region. Second, not all variation in saliva production among patients could be explained by the radiation dose (31). Third, the saliva production response of individual salivary glands may have been obscured by compensatory responses of other glands, diluting the dose-effect relationship. Finally, in addition to degeneration of the salivary gland due to loss of stem cells, other mechanisms such as fibrosis may have contributed to salivary gland dysfunction.

Together, our data show a non-uniform distribution of stem/progenitor cells in salivary glands that has consequences for radiotherapy. Radiotherapy may have similar consequences in other organs containing stem cells (32, 33) depending on the location of the stem cells and the radiation field, suggesting that optimization of the radiation field may lead to a reduction in radiation toxicity for these organs as well.

MATERIALS AND METHODS

Study design

Here, stem cell localization and consequences of stem cell irradiation were assessed in the parotid gland of mouse, rats, and human patients with head and neck cancer. The possibility of using this knowledge to further optimize radiotherapy treatment for head and neck cancer was estimated.

We assessed stem cell localization, quantity, and quality in mouse, rat, and human parotid glands. We examined the following: (i) morphology of the anatomical structures within the parotid gland using c-Kit as a stem cell marker ($n = 3$ per species); (ii) automated quantification of the number of stem cell marker–expressing cells in the rat parotid gland using tissue FAXS; (iii) qualitative assessment of stem cell potency using a sphere-forming assay. We then explored the impact of stem cell sensitivity in different areas of the rat parotid gland. We irradiated different subvolumes of the rat parotid gland using an accurate proton beam, and saliva flow was measured ($5 \leq n \leq 14$ per irradiated volume) as a read-out of parotid gland function.

To investigate the degenerative/regenerative response, we assessed slices of 50% irradiated parotid gland tissue for microscopic changes. Two irradiated and one control rat parotid glands were assessed qualitatively. Translation to patients was performed in a retrospective cohort study. In this cohort ($N = 74$), the subvolume most predictive of posttreatment function was determined in a cross-validation analysis and used to generate a predictive model that could be used to estimate posttreatment saliva production related to irradiated dose/area. A treatment planning comparative study was developed to assess the dosimetric gain that could be achieved by adding specific optimization. The potential improvement in saliva production was estimated for 22 individual patients. Histological assessments were performed blinded for tissue origin (Fig. 1). Measurement of rat parotid gland saliva production was performed unblinded (Fig. 2).

Salivary gland sphere assay

After dissection, parotid gland tissue was collected into Hanks' balanced salt solution (Gibco) containing 1% bovine serum albumin (Gibco). For rat parotid gland salisphere culture, the outer lobes of the glands were cut free from inner portions. "Outer" and "inner" portions were then processed separately. Resultant spheres from both outer and inner portions of the parotid gland were enumerated on days 3 and 6 after isolation. For more details, see Supplementary Methods.

Three-dimensional organoid differentiation

Spheres from rat parotid gland cells were trypsinized to single cells, washed, filtered, and centrifuged. They were then resuspended in medium and BD Matrigel in a concentration of 10,000 cells per gel in 12-well plates. After hardening the matrix, medium was added. Secondary spheres formed from one cell were followed for differentiation into organoid formation. For more details, see Supplementary Methods.

Rat parotid gland irradiation

The rats were anesthetized and placed in a holder hanging on a positioning rod by their upper incisors (32). Both parotid glands were irradiated with 150 MeV protons using the previously published (33–35) shoot-through technique. For more details, see Supplementary Methods and figs. S15 to S24.

Rat parotid gland function and histopathology

Stimulated saliva flow rate was determined 14 days before and up to 360 days after irradiation by a previously described procedure (24). Briefly, stimulated saliva samples of both left and right parotid glands were collected for 30 min after stimulation with pilocarpine (2 mg/kg) administered subcutaneously using miniaturized Lashley cups. Saliva flow rate (in μl/min) was calculated from the volume and actual collecting time.

At 1 year after irradiation, rats were euthanized. Both parotid glands were carefully freed from surrounding tissues, taken out, and fixated. Tissues were embedded, and 2-mm sections were cut. The sections were stained with H&E. For more details, see Supplementary Methods.

Predictive power of local dose for late function

To test whether also in humans salivary gland function depends on dose to a specific volume, a set of 74 patients treated with radiotherapy only for non–salivary gland–localized head and neck cancer were selected from a prospective cohort study performed at the British Columbia Cancer Agency, Vancouver, in which whole-mouth stimulated saliva was measured before and 1 year after radiotherapy (29). Pretreatment saliva production was required to be >5 and <12 ml in 5 min to reduce uncertainties in posttreatment relative flow calculations. This resulted in a cohort of 74 patients.

Both parotid glands were contoured in the CT scan used for radiotherapy treatment planning. From the contoured glands, we defined truncated subvolumes in the six main orthogonal directions, that is, the percentile most caudal, cranial, anterior, posterior, medial,

and lateral volumes. For given percentiles, the intersection of these truncated subvolumes defined a central subvolume of the parotid gland in three dimensions (fig. S1).

The relation between mean dose to the specified subvolumes in both glands and relative flow was modeled (details in Supplementary Methods). We determined the subvolume that minimized the error in predicted relative flow in a repeated 10-fold cross-validation scheme. Subsequently, the model for the optimized subvolume was validated by comparison of the prediction error of relative flow in a fivefold cross-validation scheme. Eventually, to optimally use the information available from the data, the final model parameter a was determined by fitting to the whole data set.

Treatment planning comparison

We hypothesized that the radiation dose to the sensitive region of the parotid gland, containing the main excretory ducts (Fig. 5), can be reduced with currently available technology. To test the hypothesis that the radiation dose to the sensitive region of the parotid gland can be reduced with currently available technology, we performed a comparative treatment planning study in 20 consecutive head and neck cancer patients treated at the radiation oncology department of the University Medical Center Groningen. For each patient, two IMRT plans with a simultaneous integrated boost were created comprising 70 Gy to the planning target volume and 54.25 Gy to the prophylactic lymph node regions in both sides of the neck.

The first plan was aimed at minimizing the mean dose to the whole parotid gland. The second plan was additionally minimized dose to the sensitive stem cell regions. The treatment plans were constructed conforming to clinical practice, including planning objectives for the targets, aiming at uniform dose distributions according to the dose prescriptions, and planning objectives for the organs at risk (table S2).

Because interplanner variations may complicate an objective comparison of treatment planning strategies, treatment plans were optimized using computerized multicriteria optimization. For a detailed description, see Supplementary Methods.

Statistics

Error bars represent the SEM. For details on the analysis of the clinical data (Fig. 5), see Supplementary Methods.

Differences in sphere formation (Fig. 1H) were tested using Student's *t* test for paired samples. Deviation from equality between irradiated and damaged volume was tested using Student's *t* test for unpaired samples. Results were considered statistically significant if $P < 0.05$.

Supplementary Material

Refer to Web version on PubMed Central for supplementary material.

Acknowledgments

We thank G. de Haan, O. C. M. Sibon, and H. H. Kampinga for suggestions to improve the manuscript. Part of the work has been performed at the UMCG (University Medical Center Groningen) Microscopy and Imaging Center (UMIC), which is sponsored by the Netherlands Organization for Scientific Research (NWO) grants 40-00506-98-9021 and 175-010-2009-023.

Funding: Supported by grant no. 916.76.029 from the Innovational Research Incentives Scheme of the NWO; RuG 2002-2673, RuG 2008-4022, and Rug 2013-5792 of the Dutch Cancer Society; and ZonMw grant number 11.600.1023.

REFERENCES AND NOTES

1. Bentzen SM. Preventing or reducing late side effects of radiation therapy: Radiobiology meets molecular pathology. Nat Rev Cancer. 2006; 6:702–713. [PubMed: 16929324]
2. Langendijk JA, Doornaert P, Verdonck-de-Leeuw IM, Leemans CR, Aaronson NK, Slotman BJ. Impact of late treatment-related toxicity on quality of life among patients with head and neck cancer treated with radiotherapy. J Clin Oncol. 2008; 26:3770–3776. [PubMed: 18669465]
3. Dirix P, Nuyts S. Evidence-based organ-sparing radiotherapy in head and neck cancer. Lancet Oncol. 2010; 11:85–91. [PubMed: 20129131]
4. Sciubba JJ, Goldenberg D. Oral complications of radiotherapy. Lancet Oncol. 2006; 7:175–183. [PubMed: 16455482]
5. Rischin D, Corry J, Smith J, Stewart J, Hughes P, Peters L. Excellent disease control and survival in patients with advanced nasopharyngeal cancer treated with chemoradiation. J Clin Oncol. 2002; 20:1845–1852. [PubMed: 11919243]
6. Vissink A, Jansma J, Spijkervet FK, Burlage FR, Coppes RP. Oral sequelae of head and neck radiotherapy. Crit Rev Oral Biol Med. 2003; 14:199–212. [PubMed: 12799323]
7. Brockstein BE, Vokes EE. Head and neck cancer in 2010: Maximizing survival and minimizing toxicity. Nat Rev Clin Oncol. 2011; 8:72–74. [PubMed: 21278773]
8. Bohuslavizki KH, Klutmann S, Brenner W, Mester J, Henze E, Clausen M. Salivary gland protection by amifostine in high-dose radioiodine treatment: Results of a double-blind placebo-controlled study. J Clin Oncol. 1998; 16:3542–3549. [PubMed: 9817273]
9. Brizel DM, Wasserman TH, Henke M, Strnad V, Rudat V, Monnier A, Eschwege F, Zhang J, Russell L, Oster W, Sauer R. Phase III randomized trial of amifostine as a radioprotector in head and neck cancer. J Clin Oncol. 2000; 18:3339–3345. [PubMed: 11013273]
10. LeVeque FG, Montgomery M, Potter D, Zimmer MB, Rieke JW, Steiger BW, Gallagher SC, Muscoplat CC. A multicenter, randomized, double-blind, placebo-controlled, dose-titration study of oral pilocarpine for treatment of radiation-induced xerostomia in head and neck cancer patients. J Clin Oncol. 1993; 11:1124–1131. [PubMed: 8501499]
11. Burlage FR, Roesink JM, Kampinga HH, Coppes RP, Terhaard C, Langendijk JA, van Luijk P, Stokman MA, Vissink A. Protection of salivary function by concomitant pilocarpine during radiotherapy: A double-blind, randomized, placebo-controlled study. Int J Radiat Oncol Biol Phys. 2008; 70:14–22. [PubMed: 17869018]
12. Feng FY, Kim HM, Lyden TH, Haxer MJ, Worden FP, Feng M, Moyer JS, Prince ME, Carey TE, Wolf GT, Bradford CR, Chepeha DB, Eisbruch A. Intensity-modulated chemoradiotherapy aiming to reduce dysphagia in patients with oropharyngeal cancer: Clinical and functional results. J Clin Oncol. 2010; 28:2732–2738. [PubMed: 20421546]
13. Eisbruch A. Radiotherapy: IMRT reduces xerostomia and potentially improves QoL. Nat Rev Clin Oncol. 2009; 6:567–568. [PubMed: 19787001]
14. Kam MKM, Leung SF, Zee B, Chau RMC, Suen JJS, Mo F, Lai M, Ho R, Cheung KY, Yu BKH, Chiu SKW, Choi PHK, Teo PML, Kwan WH, Chan ATC. Prospective randomized study of intensity-modulated radiotherapy on salivary gland function in early-stage nasopharyngeal carcinoma patients. J Clin Oncol. 2007; 25:4873–4879. [PubMed: 17971582]
15. Nutting CM, Morden JP, Harrington KJ, Urbano TG, Bhide SA, Clark C, Miles EA, Miah AB, Newbold K, Tanay M, Adab F, Jefferies SJ, Scrase C, Yap BK, A'Hern RP, Sydenham MA, Emson

M, Hall E, PARSPORT trial management group. Parotid-sparing intensity modulated versus conventional radiotherapy in head and neck cancer (PARSPORT): A phase 3 multicentre randomised controlled trial. Lancet Oncol. 2011; 12:127–136. [PubMed: 21236730]

16. Murdoch-Kinch CA, Kim HM, Vineberg KA, Ship JA, Eisbruch A. Dose-effect relationships for the submandibular salivary glands and implications for their sparing by intensity modulated radiotherapy. Int J Radiat Oncol Biol Phys. 2008; 72:373–382. [PubMed: 18337023]
17. Dijkema T, Raaijmakers CPJ, Ten Haken RK, Roesink JM, Braam PM, Houweling AC, Moerland MA, Eisbruch A, Terhaard CHJ. Parotid gland function after radiotherapy: The combined Michigan and Utrecht experience. Int J Radiat Oncol Biol Phys. 2010; 78:449–453. [PubMed: 20056347]
18. Jellema AP, Doornaert P, Slotman BJ, Leemans CR, Langendijk JA. Does radiation dose to the salivary glands and oral cavity predict patient-rated xerostomia and sticky saliva in head and neck cancer patients treated with curative radiotherapy? Radiother Oncol. 2005; 77:164–171. [PubMed: 16256229]
19. Deasy JO, Moiseenko V, Marks L, Chao KS, Nam J, Eisbruch A. Radiotherapy dose–volume effects on salivary gland function. Int J Radiat Oncol Biol Phys. 2010; 76:S58–S63. [PubMed: 20171519]
20. Braam PM, Roesink JM, Moerland MA, Raaijmakers CPJ, Schipper M, Terhaard CHJ. Long-term parotid gland function after radiotherapy. Int J Radiat Oncol Biol Phys. 2005; 62:659–664. [PubMed: 15936542]
21. Li Y, Taylor JM, Ten Haken RK, Eisbruch A. The impact of dose on parotid salivary recovery in head and neck cancer patients treated with radiation therapy. Int J Radiat Oncol Biol Phys. 2007; 67:660–669. [PubMed: 17141973]
22. Lombaert IM, Brunsting JF, Wierenga PK, Kampinga HH, de Haan G, Coppes RP. Keratinocyte growth factor prevents radiation damage to salivary glands by expansion of the stem/progenitor pool. Stem Cells. 2008; 26:2595–2601. [PubMed: 18669914]
23. Lombaert IMA, Brunsting JF, Wierenga PK, Faber H, Stokman MA, Kok T, Visser WH, Kampinga HH, de Haan G, Coppes RP. Rescue of salivary gland function after stem cell transplantation in irradiated glands. PLOS One. 2008; 3:e2063. [PubMed: 18446241]
24. Konings AWT, Cotteleer F, Faber H, van Luijk P, Meertens H, Coppes RP. Volume effects and region-dependent radiosensitivity of the parotid gland. Int J Radiat Oncol Biol Phys. 2005; 62:1090–1095. [PubMed: 15990013]
25. van Luijk P, Faber H, Schippers JM, Brandenburg S, Langendijk JA, Meertens H, Coppes RP. Bath and shower effects in the rat parotid gland explain increased relative risk of parotid gland dysfunction after intensity-modulated radiotherapy. Int J Radiat Oncol Biol Phys. 2009; 74:1002–1005. [PubMed: 19545785]
26. Nanduri LS, Maimets M, Pringle SA, van der Zwaag M, van Os RP, Coppes RP. Regeneration of irradiated salivary glands with stem cell marker expressing cells. Radiother Oncol. 2011; 99:367–372. [PubMed: 21719134]
27. Nanduri LSY, Baanstra M, Faber H, Rocchi C, Zwart E, de Haan G, van Os RP, Coppes RP. Purification and ex vivo expansion of fully functional salivary gland stem cells. Stem Cell Rep. 2014; 3:957–964.
28. Konings AW, Faber H, Cotteleer F, Vissink A, Coppes RP. Secondary radiation damage as the main cause for unexpected volume effects: A histopathologic study of the parotid gland. Int J Radiat Oncol Biol Phys. 2006; 64:98–105. [PubMed: 16226398]
29. Moiseenko V, Wu J, Hovan A, Saleh Z, Apte A, Deasy JO, Harrow S, Rabuka C, Muggli A, Thompson A. Treatment planning constraints to avoid xerostomia in head-and-neck radiotherapy: An independent test of QUANTEC criteria using a prospectively collected dataset. Int J Radiat Oncol Biol Phys. 2012; 82:1108–1114. [PubMed: 21640505]
30. Xiao N, Lin Y, Cao H, Sirjani D, Giaccia AJ, Koong AC, Kong CS, Diehn M, Le Q-T. Neurotrophic factor GDNF promotes survival of salivary stem cells. J Clin Invest. 2014; 124:3364–3377. [PubMed: 25036711]
31. Chao KS, Deasy JO, Markman J, Haynie J, Perez CA, Purdy JA, Low DA. A prospective study of salivary function sparing in patients with head-and-neck cancers receiving intensity-modulated or

three-dimensional radiation therapy: Initial results. Int J Radiat Oncol Biol Phys. 2001; 49:907–916. [PubMed: 11240231]

32. Cotteleer F, Faber H, Konings AW, Van der Hulst PC, Coppes RP, Meertens H. Three-dimensional dose distribution for partial irradiation of rat parotid glands with 200 kV X-rays. Int J Radiat Biol. 2003; 79:689–700. [PubMed: 14703942]
33. van Luijk P, Bijl HP, Coppes RP, van der Kogel AJ, Konings AW, Pikkemaat JA, Schippers JM. Techniques for precision irradiation of the lateral half of the rat cervical spinal cord using 150 MeV protons. Phys Med Biol. 2001; 46:2857–2871. [PubMed: 11720351]
34. van Luijk P, van t'Veld AA, Zelle HD, Schippers JM. Collimator scatter and 2D dosimetry in small proton beams. Phys Med Biol. 2001; 46:653–670. [PubMed: 11277215]
35. Boon SN, van Luijk P, Schippers JM, Meertens H, Denis JM, Vynckier S, Medin J, Grusell E. Fast 2D phantom dosimetry for scanning proton beams. Med Phys. 1998; 25:464–475. [PubMed: 9571612]

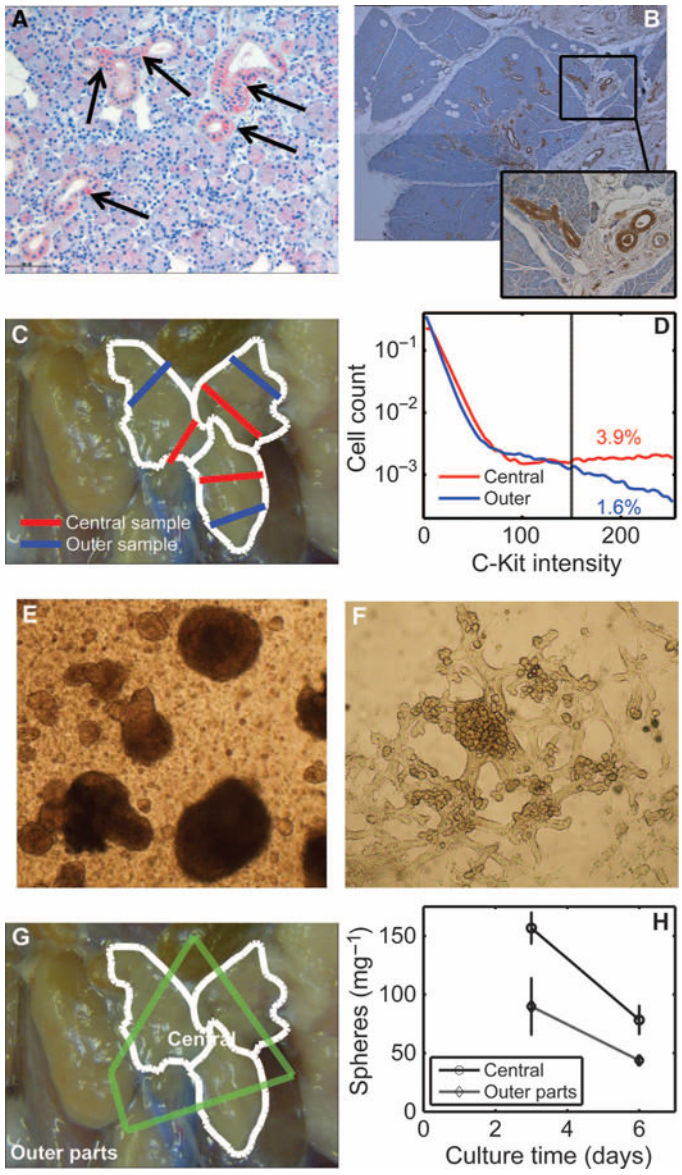

Fig. 1. Localization of stem/progenitor cells in human and rat salivary glands

(**A** and **B**) In the human (A) and rat (B) salivary glands, c-Kit^{+} stem cells were predominantly found in the larger ducts. (**C**) In the rat parotid gland, the main ducts connected the three lobes and were located centrally. The fraction of cells with the highest expression of c-Kit was found in the central parts of each lobe compared to the outer parts. (**D**) Stem/progenitor cells expressing c-Kit. (**E**) Cells formed spheres after several days in culture. (**F**) These cells developed into gland-like structures containing ducts and acini. (**G**) Depiction of the center and outer regions of the rat parotid gland. (**H**) Number of cells from the central and outer parts of the rat parotid gland capable of forming spheres after culture. Error bars indicate the SEM.

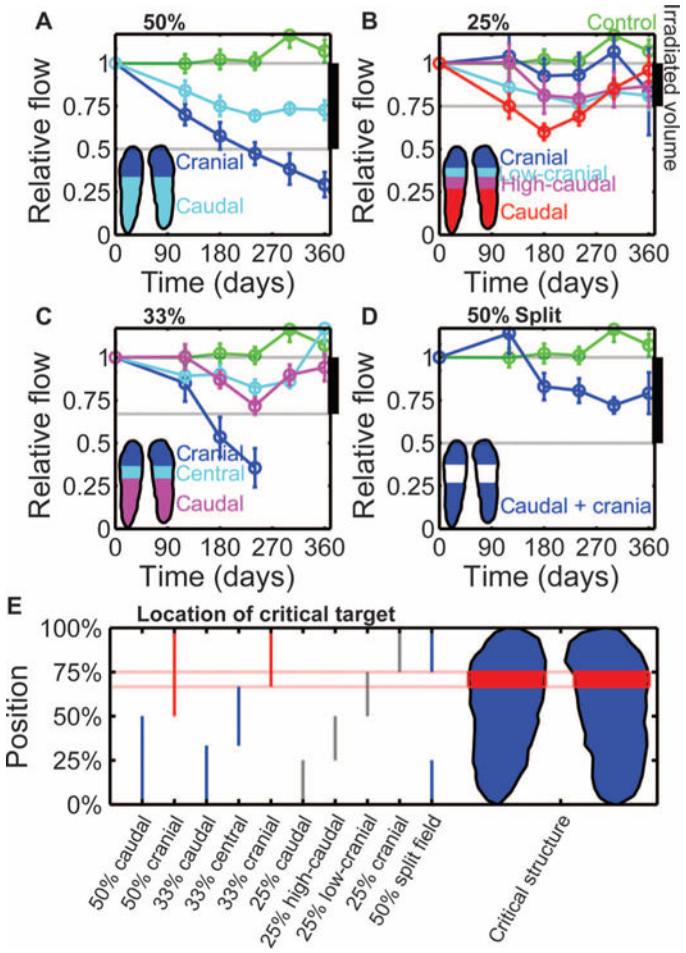

Fig. 2. Region-dependent radiosensitivity of the rat parotid gland

(**A** to **D**) Relative residual stimulated saliva flow rate after irradiation of various subvolumes of the rat parotid gland. The green line indicates the relative saliva flow rate of the non-irradiated control animals over time. The stippled line indicates the expected loss of function if the irradiated volume of the rat parotid gland is assumed to lose all function. Irradiation of the rat parotid gland—cranial 50% (A, blue subvolume) or 33% (C, blue subvolume)—led to loss of function. Including the cranial 25% (D, blue subvolume) of the rat parotid gland in a 50% split field configuration led to a less-than-proportional response. Irradiating 25% of the parotid gland did not induce durable loss of function (B). (**E**) Overview of irradiated subvolumes. When the irradiated volume exceeded 25%, there was irreversible damage to the salivary gland [red or blue lines in (E)]. Error bars indicate the SEM.

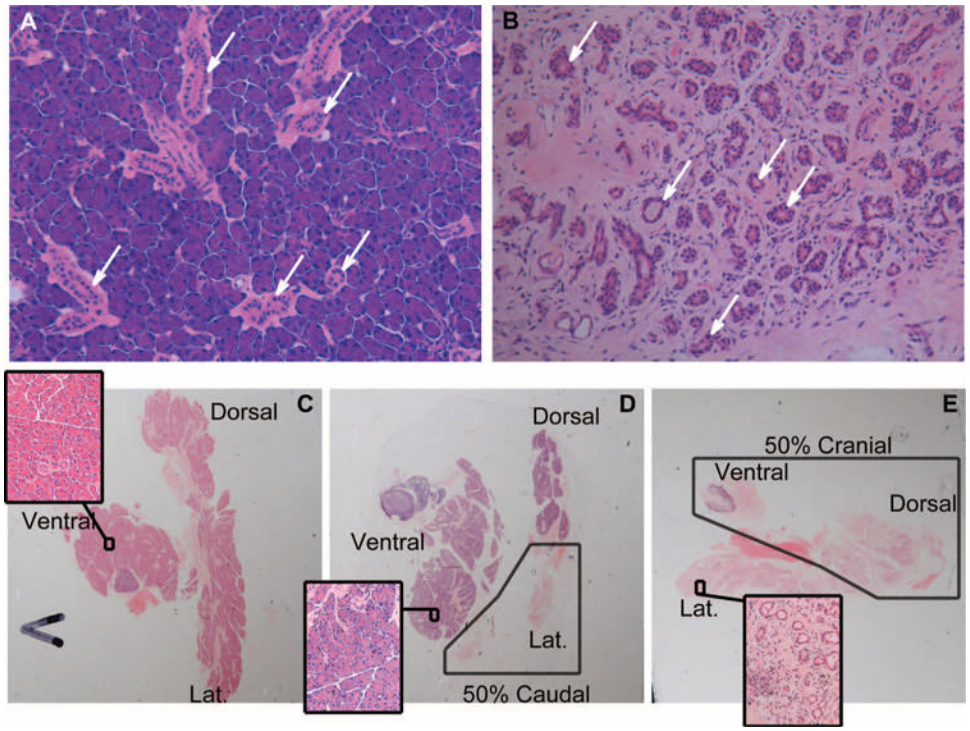

Fig. 3. Damage to rat parotid gland depends on the dose to the critical region

(**A** and **B**) Normal (A) and irradiated (B) rat parotid gland tissues. The white arrows indicate the position of salivary gland ducts. (**C**) Non-irradiated hematoxylin and eosin (H&E)–stained rat parotid gland. (**D** and **E**) Fifty percent irradiated rat parotid glands; black line indicates estimated position of the edge of the radiation field. (D) Irradiation of the caudal 50% of the rat parotid gland spared the critical region identified in Fig. 2; the irradiated parts of the lateral (Lat.) and ventral lobes degenerated but without visible damage to the non-irradiated sections. (E) Irradiation of the cranial 50% of the rat parotid gland, which includes the critical region containing stem/progenitor cells, led to degeneration of all lobes, including the non-irradiated sections.

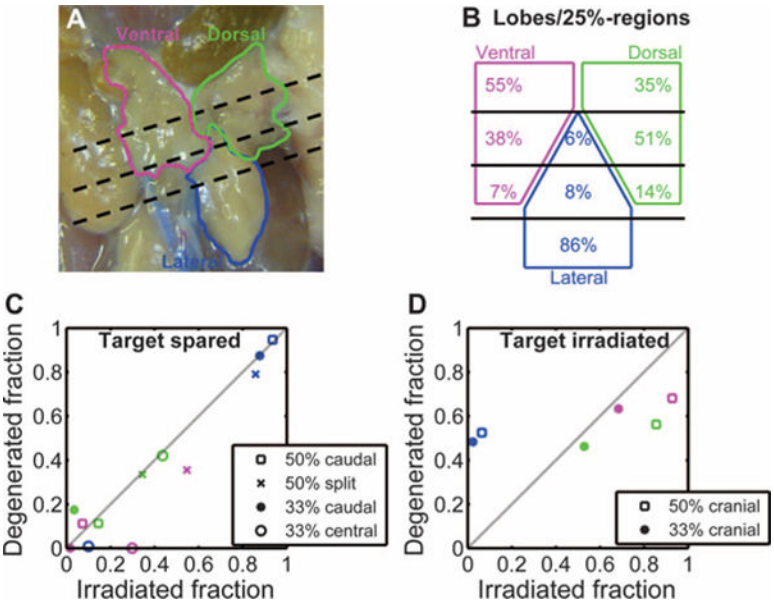

Fig. 4. Irradiation of the critical region results in damage independent of the irradiated fraction

By relating the fraction of degenerated tissue in each lobe to the dose distribution, the fraction of each lobe contained in the radiation field could be estimated for all fields. (**A** and **B**) The dashed black line indicates the field edges for all non-overlapping 25% irradiated regions. (**C**) For fields not containing the critical region, the damaged volume per lobe corresponded to the irradiated volume per lobe. (**D**) In contrast, the response to fields containing the critical region (33 and 50% cranial fields) is not related to the irradiated volume.

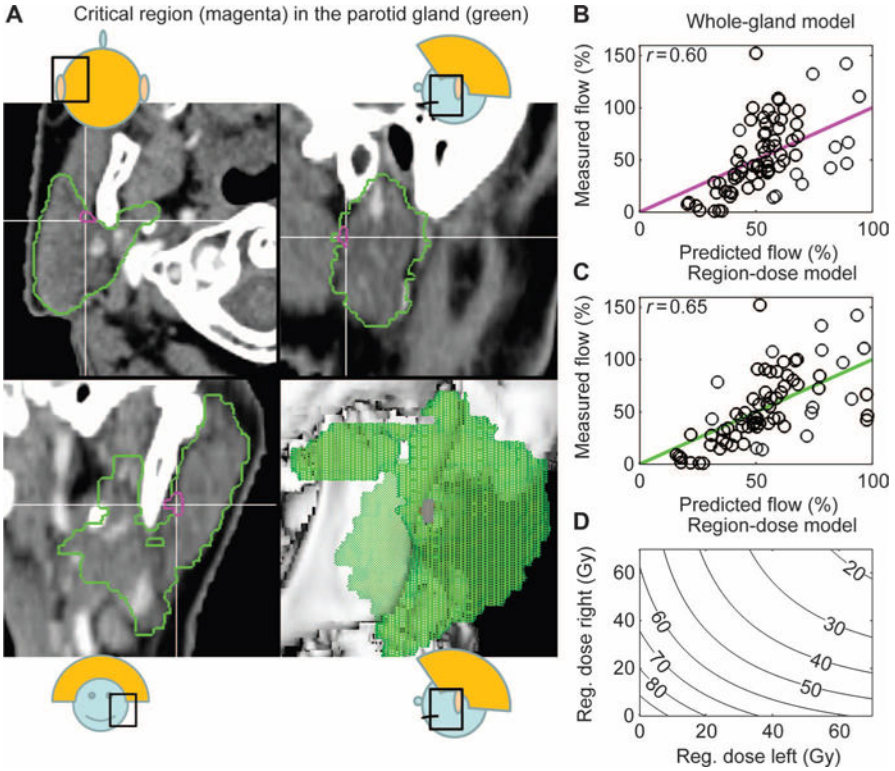

Fig. 5. The radiation dose to human parotid gland substructures predicted loss of saliva production

Saliva production 1 year after radiotherapy was related to the radiation dose administered to specific subvolumes of the gland. (**A**) Critical subvolume (magenta) within the parotid gland (green). (**B** and **C**) Dose to this subvolume most strongly correlated with post-treatment saliva production. (**D**) Prediction of total saliva production at 1 year after radiotherapy based on the dose to the critical subvolumes of both parotid glands.

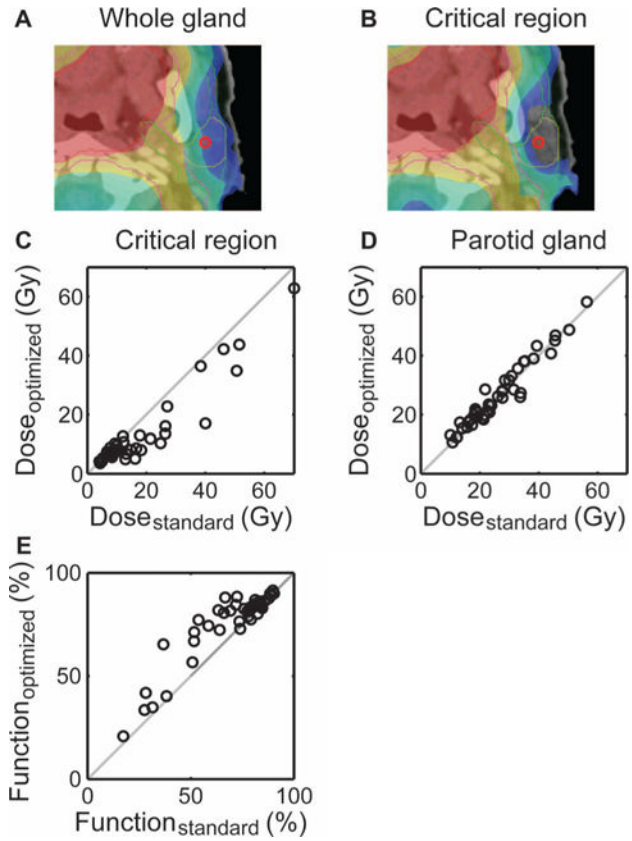

Fig. 6. Sparing the critical region of the human parotid gland after IMRT

(**A** and **B**) Minimizing the dose to the critical region (red circle) of the human parotid gland was predicted to result in a redistribution of dose within the parotid glands. (**C** to **E**) This optimization was performed on data from 22 patients with head and neck cancer and was predicted to result in a reduction of dose to the critical region (C and E), with minimal or no change to the mean dose to the whole parotid gland (D).